Supporting Information

Molecular dynamics simulations provide insight into possible role of ladderane structures in anammox bacteria

Terezie Císařová[1], Martin Balouch[1,2], Jaroslav Hanuš[1], Karel Berka[3], Vojtěch Kouba[4], František Štěpánek[1*]

[1]Department of Chemical Engineering, University of Chemistry and Technology Prague, Technická 5, Prague 6 166 28, Czech Republic

[2]Zentiva, k.s., U Kabelovny 130, Prague 10 102 37, Czech Republic

[3]Department of Physical Chemistry, Faculty of Science, Palacký University Olomouc, 17. listopadu 12, Olomouc 771 46, Czech Republic

[4]Department of Water Technology and Environmental Engineering, University of Chemistry and Technology Prague, Technická 5, 166 28 Prague, Czechia

[*]Corresponding author. E-mail: stepanef@vscht.cz; tel.: +420 220 443 165

Table S1: Overview of all simulated systems. Each system consists of 128 lipid molecules; systems highlighted in blue were additionally simulated at 512 lipids.

DPPC-LA35 bilayers	DPPC content (%)	LA35 content (%)	Other
0 %	100	0	—
17 %	83	17	—
33 %	67	33	—
50 %	50	50	—
66 %	34	66	—
78 %	22	78	—
83 %	17	83	—
100 %	0	100	—
Bacterially derived lipids - IPPC	**DPPC content (%)**	**LA35 content (%)**	**IPPC content (%)**
0 %	—	0	100
17 %	—	17	83
50 %	—	50	50
83 %	—	83	17
100 %	—	100	0

Different ladderane lipids and alcohols	DPPC content (%)	LA35 content (%)	Other
LA35	78	22	—
LA55	78	—	22 % LA55
6OL3	78	—	22 % 6OL3
6OL5	78	—	22 % 6OL5
CHOL	78	—	22 % CHOL

SI.1 Input files creation

The topology input files for ladderane alcohols were created by modifying the provided input files for ladderane phospholipids as follows:

1. The .itp file for the LA35 molecule was altered to retain only the relevant bonds, angles, and dihedral angles found in the alcohol molecule.
2. One hydrogen atom was removed from the terminal carbon, and the carbon atom was converted into an oxygen atom.
3. This oxygen atom was assigned a suitable atom type from the CHARMM36 force field to reflect its hydroxyl nature.
4. The charges of the molecules neighbouring the oxygen atom were adjusted accordingly to ensure overall charge neutrality.
5. Finally, all atoms were renumbered.
6. The .pdb and .itp files for cholesterol and DPPC molecules were obtained from CHARMM-GUI.

A custom Python script was utilised to create a .pdb input file (script layout in Fig. S1) containing the coordinates of a phospholipid bilayer with 128 molecules (64 per leaflet). A total of 6712 TIP3P water molecules were added using integrated GROMACS functions.

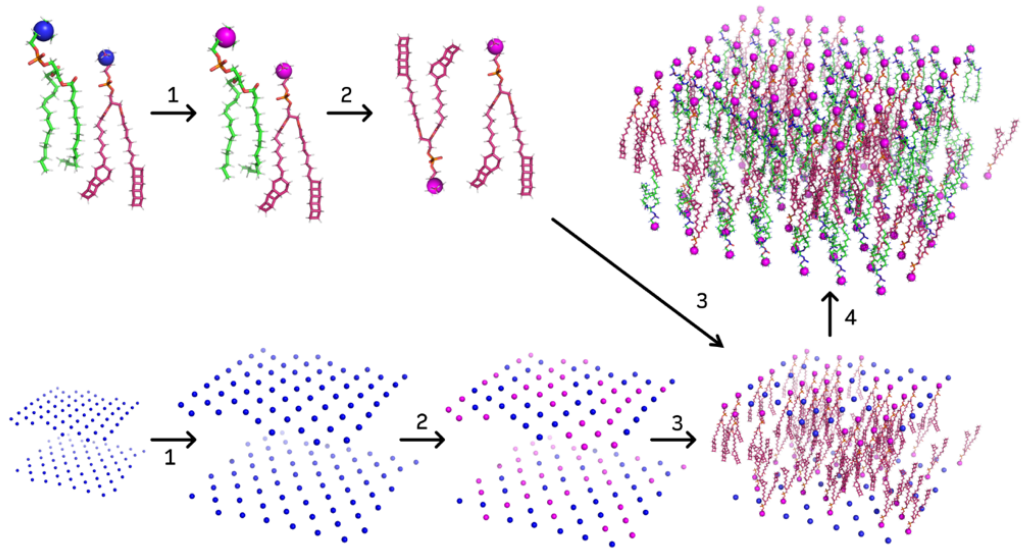

Figure S1: Visualisation of the bilayer creation process: 1 - scaling of the template and choice of a headgroup atom, 2 - rotation of phospholipid models to obtain a template for both leaflets, random assignment of one molecule-type to the template positions, 3 - transferring whole molecules of one phospholipid type to their assigned positions in the template, 4 - repeat for other molecule-types.

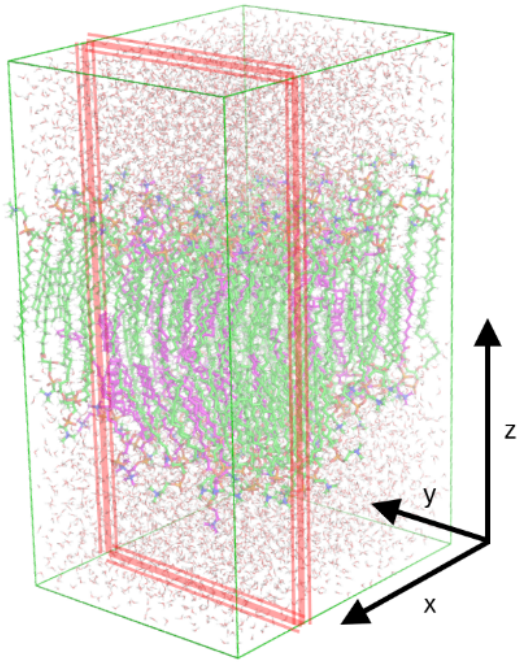

Figure S2: Visualisation coordinate convention of the simulated bilayers. The sampling frame used for bilayer structure visualisation is indicated by the red border.

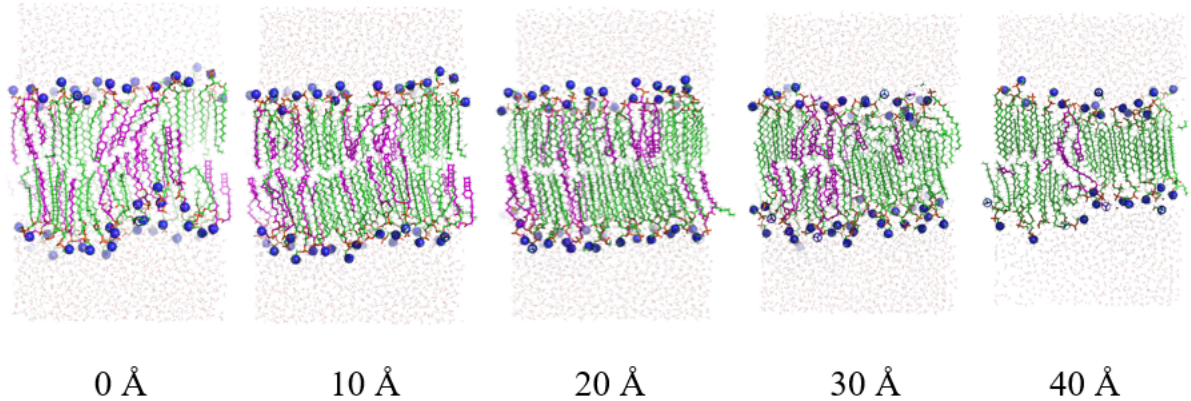

Figure S3: Sliced representations of the final state of a DPPC bilayer containing 22 % LA35. Each slice spans 20 Å in width, with the corresponding distances from the first slice indicated. An ordered region is visible at distances of 10 and 20 Å, while a ripple-like region appears at 40 Å.

SI.2 Size dependence

For better comparison, results obtained for bilayers four times larger are presented. As can be seen, the phase behaviour of all systems is very similar; just the bilayer rippling also occurs at lower LA35 contents (comparing Fig. 3 and Fig. S4). The most pronounced difference is observed in the thickness analysis, where thickness variations are significantly larger in the bigger systems (Fig. S5). This is expected, as larger bilayers provide a greater lateral area for the development of undulations, caused in part by the presence of rippled regions. Otherwise, the overall behaviour is consistent with that of the smaller systems, whose analyses and results are presented in the main text.

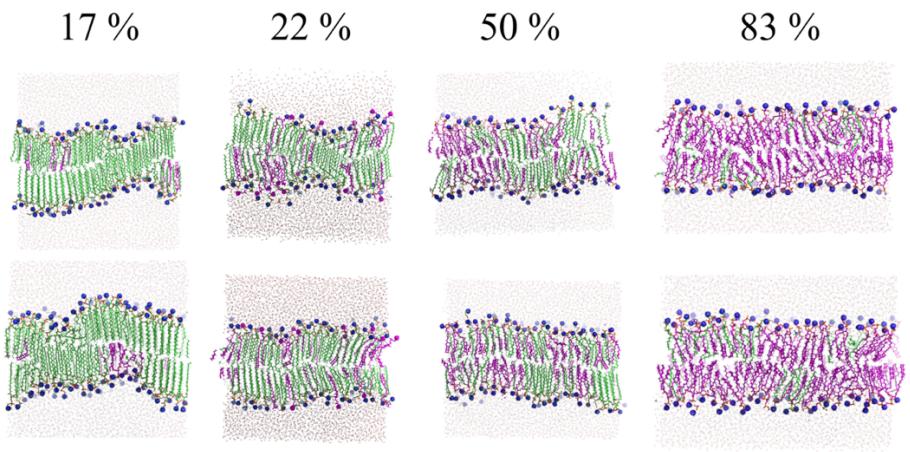

Figure S4: Final states of DPPC-LA35 bilayers obtained by MD simulations using an enlarged system (512 molecules), represented by 20 Å wide cross-sectional slices in two orthogonal directions for each case. The values indicate the molar percentage of LA35 in the bilayer. DPPC molecules are shown in green, LA35 molecules in magenta, and nitrogen atoms in blue.

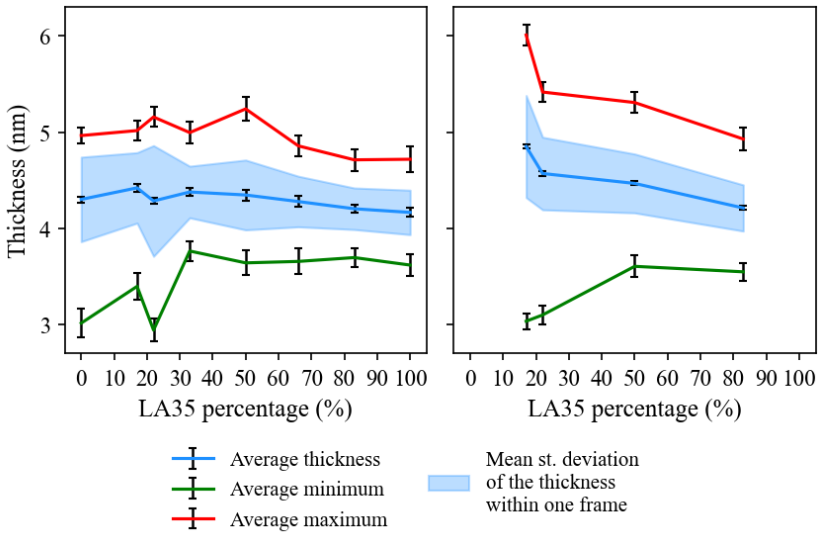

Figure S5: Membrane thickness as a function of LA35 percentage in the membrane in small (left) and 4 times bigger systems (right). The error bars represent the standard deviation of the average thickness values of the last 50 ns of the MD simulation, and the blue region signifies the mean standard deviation within one bilayer conformation.

SI.3 Molecular grouping

To investigate potential phase separation curves representing the ratio of intermolecular contacts between minority components (x_{minmin}) in each leaflet were plotted. As a contact, an intermolecular distance < 0.4 nm is classified. The value of 100 % corresponds to the sum of all contacts with the minority group, including both minority–minority (n_{minmin}) and minority–majority (n_{minmaj}) contacts.

$$x_{minmin} = \frac{n_{minmin}}{n_{minmin} + n_{minmaj}}.$$

Data were collected every 100 fs. The resulting curves were smoothed using a moving average with a window size of 25.

In the DPPC-LA35 bilayers, the minority groups differ for each bilayer. For 17 % and 22 %, the LA35 molecules are in the minority, for 66 % and 83 %, the DPPC molecules are in the minority. When LA35 molecules were in the minority, no molecular grouping or dispersion was observed. When DPPC molecules were in the minority, the ratio profile was somewhat more irregular, but this can still be attributed to random molecular motion.

In DPPC bilayers containing a fixed 22 % of ladderane molecules or cholesterol, DPPC was always in the majority. Some degree of separation may be present in the upper leaflet of the bilayer, as suggested by the x_{minmin} dependence, but otherwise no phase separation was observed within the leaflets. Among the different systems, the only significant phase separation occurred in the bilayer with 22 % LA35, where the rippling of the bilayer was formed predominantly from DPPC molecules, causing the minority LA35 molecules to concentrate in the non-rippled regions. All other x_{minmin} dependencies can be regarded as arising from random behaviour.

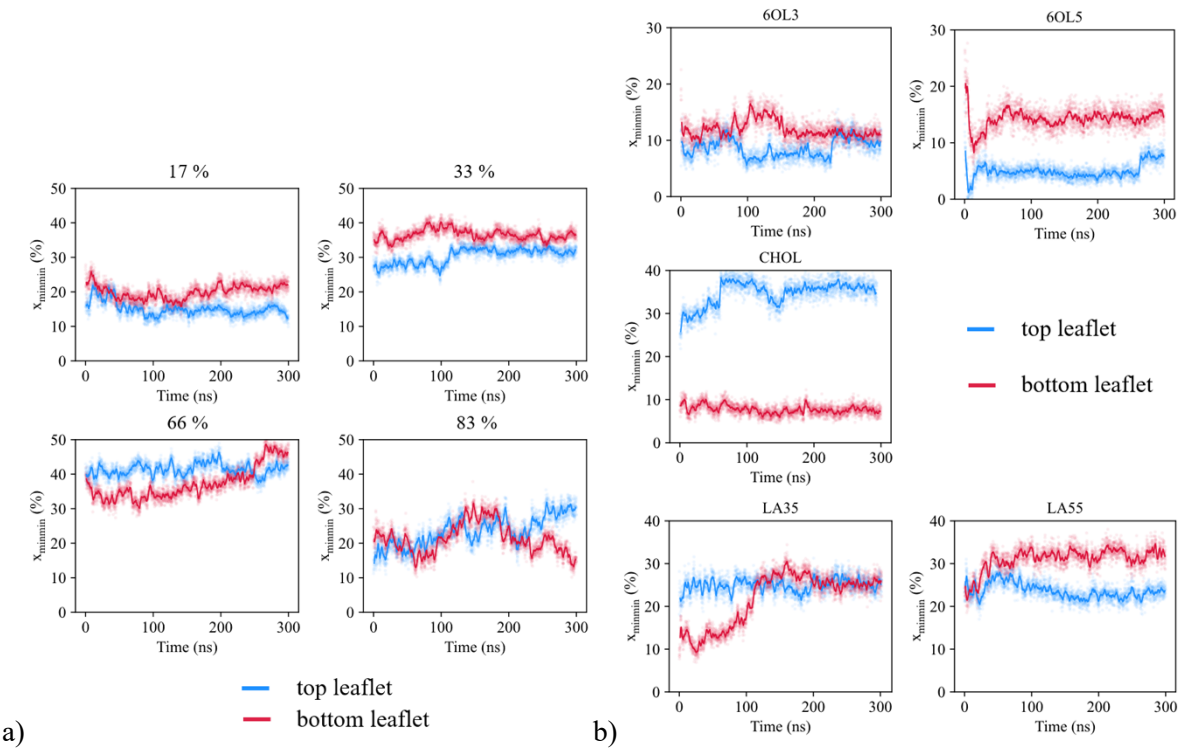

Figure S6: a) Ratio of intermolecular contacts between minority components as function of time for DPPC-LA35 bilayers with increasing percentage of LA35 as indicated. b) Ratio of intermolecular contacts between minority components as function of time for DPPC bilayers with a fixed 22 % of ladderanes of cholesterol as indicated.

SI.4 Deuterium order parameter

Carbon-hydrogen or carbon-deuterium (S_{CD}) order parameter describes the orientation (orientational mobility) of the C─H bonds in relation to the bilayer normal, conventionally the Z-axis in bilayer simulation. Its value can be computed from the all-atom system simulation by calculating the value of the C─H → Z-axis angle (notated as θ) for each carbon atom of the lipid tail accordingly[S1]:

$$S_{CD} = \frac{\langle 3\cos^2\theta - 1 \rangle}{2},$$

where ⟨ ⟩ denotes the time average. Conventionally, the $-S_{CD}$ numbers are computed by gmx order. The more the absolute value $|S_{CD}|$ approaches 0.5 (the state where the C─H bonds are parallel to the bilayer plane), the more ordered the bilayer is.

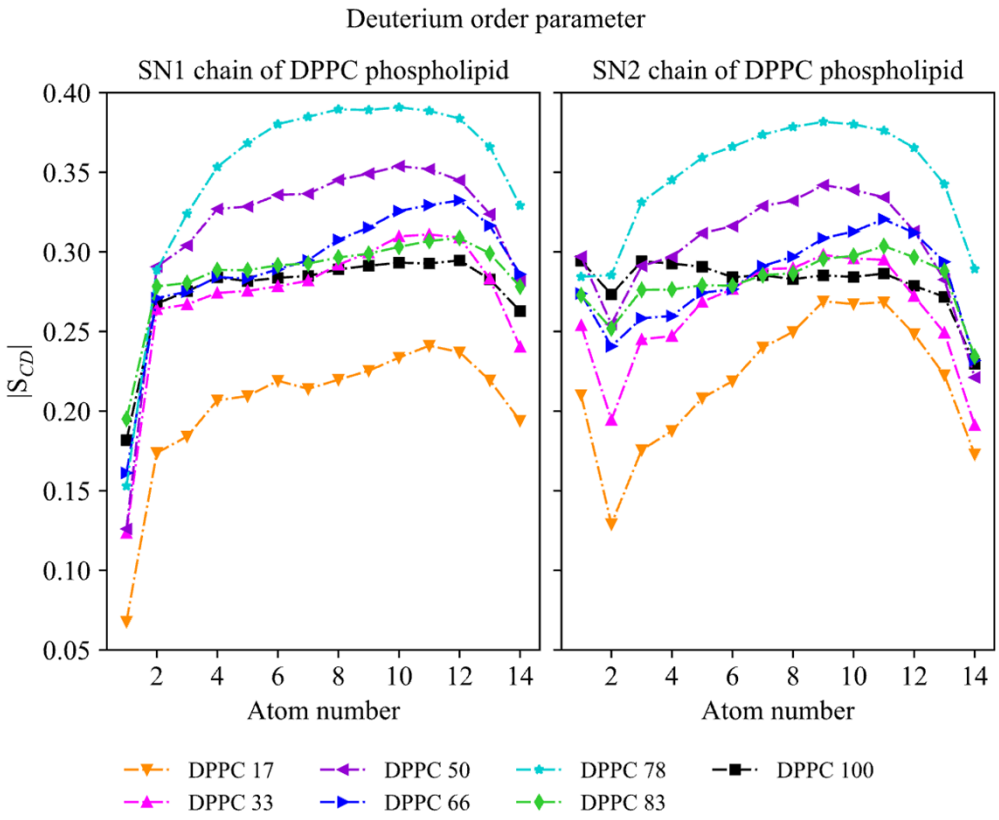

Figure S7: Deuterium order parameter for both acyl chains inside DPPC molecules for DPPC-LA35 bilayers with a varying percentage of DPPC as indicated in the legend.

In pure DPPC bilayer simulations found in the literature at room temperatures, the $-S_{CD}$ of the SN1 chain typically decreases gradually from around 0.2 with increasing distance of the carbon from the polar head.[S2] In our $|S_{CD}|$ evaluation of the SN1 chain, the pure DPPC bilayer exhibited a stable $|S_{CD}|$ value slightly below 0.3, with a sudden decrease for the last two atoms. The higher $|S_{CD}|$ value compared to existing studies is presumably attributable to the lower simulation temperature (10 °C). As for the SN2 chain, the first carbons of the SN2 acyl chain should be closer to the surface and have a higher $|S_{CD}|$ number than those in the SN1 chain (except of course for the second atom).[S3] In our case, this holds true for the sixth atom.

Unexpectedly, in both SN1 and SN2 chains, membranes DPPC 50, DPPC 66, DPPC 78 and DPPC 83 show similar or higher values of $|S_{CD}|$ compared to the pure DPPC bilayer, despite the visual inspection and area per lipid suggesting lower ordering. This inconsistency is caused by the visible parallel tilt of ordered DPPC molecules in the DPPC 100 bilayer. The tilt of the ordered DPPC bilayer is a known phenomenon and is dependent on the temperature or eventual cholesterol content.[S3,S4] Regarding bilayers DPPC 17 and DPPC 33, there is $|S_{CD}|$ increment around the 10^{th} –11^{th} atom in the SN2 chain.. Those bilayers are in an unordered state.

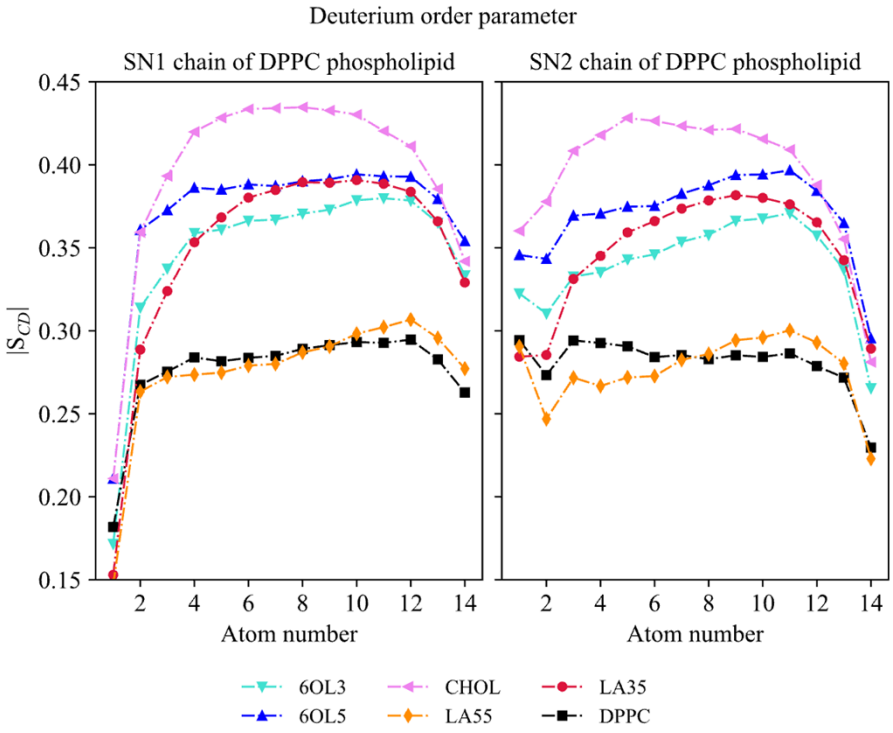

Figure S8: Deuterium order parameter for both acyl chains inside DPPC molecules for DPPC bilayers with fixed 22 % of ladderanes or cholesterol as indicated in the legend.

Regarding the deuterium order parameter, the addition of CHOL to the bilayer improved its ordering, especially for the middle carbons within the acyl chain. This is in good agreement with the literature, where upon the addition of cholesterol to the bilayer, the $|S_{CD}|$number increases from the fourth carbon, reaching a peak around the ninth carbon atom, and then slowly decreases with distance.[S3] Cholesterol molecules are known to increase the ordering of the bilayer while preserving its fluidity. As 10 °C is far below the transition temperature of DPPC bilayers, the bilayer should be either in a significantly ordered liquid state or in a gel state. (paper [S5] suggests a so-called modulated phase, which is a liquid phase with high thickness variance). The $|S_{CD}|$ values of the ladderane alcohols are lower than those of cholesterol; however, they still apparently introduce orderliness to the membrane. Surprisingly, the LA35 values are as high as the alcohol bilayers. This high ordering is caused by the rippling of the bilayer, where the rippled site in the bilayer is ordered by interlocking of the DPPC chains from opposing leaflets with no significant tilt.

SI.5 Density

Mass density profiles along the bilayer normal were created to analyse the bilayer integrity and assess the distribution of molecular density across the bilayer. This analysis offers insight into the partitioning potential of small-molecule hydrophobic substances into the membrane, as multiple regions throughout the bilayer are suitable for substance incorporation.[S6,S7]

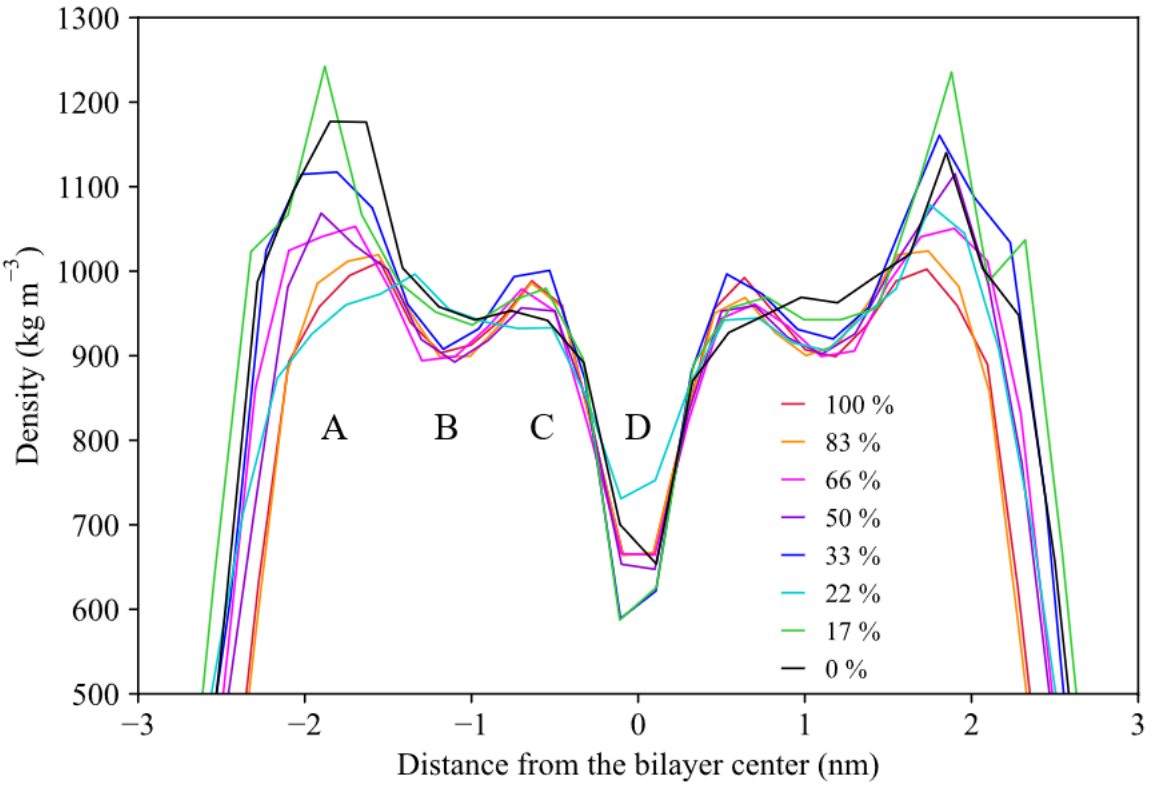

Figure S9: Density profile of LA35-DPPC bilayers through the bilayer (alongside the z-axis). A, B, C and D regions are marked. Different LA35 ratios are colour-coded.

There are four distinctive density areas in Fig. S9. Area **A** represents the phospholipid headgroups, the densest part of the bilayer, located approximately 2 nm from the centre of the bilayer. Here, the density of this region increases with higher DPPC content in the bilayer. In contrast, in the second visible maximum, approximately 0.6 nm from the bilayer centre (region **C**), where ladderane motifs are present, the bilayer density increases proportionally with the abundance of ladderane phospholipids. Area **B**, situated approximately 1.2 nm from the bilayer centre, contains a local density minimum. For bilayers with more than 22 mol% of LA35 phospholipid, this minimum is quite distinctive. The density values are very similar across these bilayers. The LA 0 bilayer exhibits a higher density in this region compared to region C. Finally, region **D** is located at 0 nm in the interleaflet cavity. Although no explicit density trend is observed in region **D**, the pure DPPC bilayer is the densest among all membranes in this area, possibly indicating that the addition of LA35 phospholipid causes disruptions and increases the spacing between leaflets.

The addition of LA35 phospholipids may enhance the incorporation of substances favouring region **D**, which are typically small hydrophobic molecules like benzene.[S8] Conversely, the increased density in area C could limit the encapsulation of larger hydrophobic molecules.[S8] However, less hydrophobic small-molecule solutes tend to incorporate beneath the phospholipid headgroups corresponding to region **B**,[S9,S10]which exhibits lower density in LA35-rich membranes. Therefore, such membranes may have more space available to act as hosts for substance encapsulation.

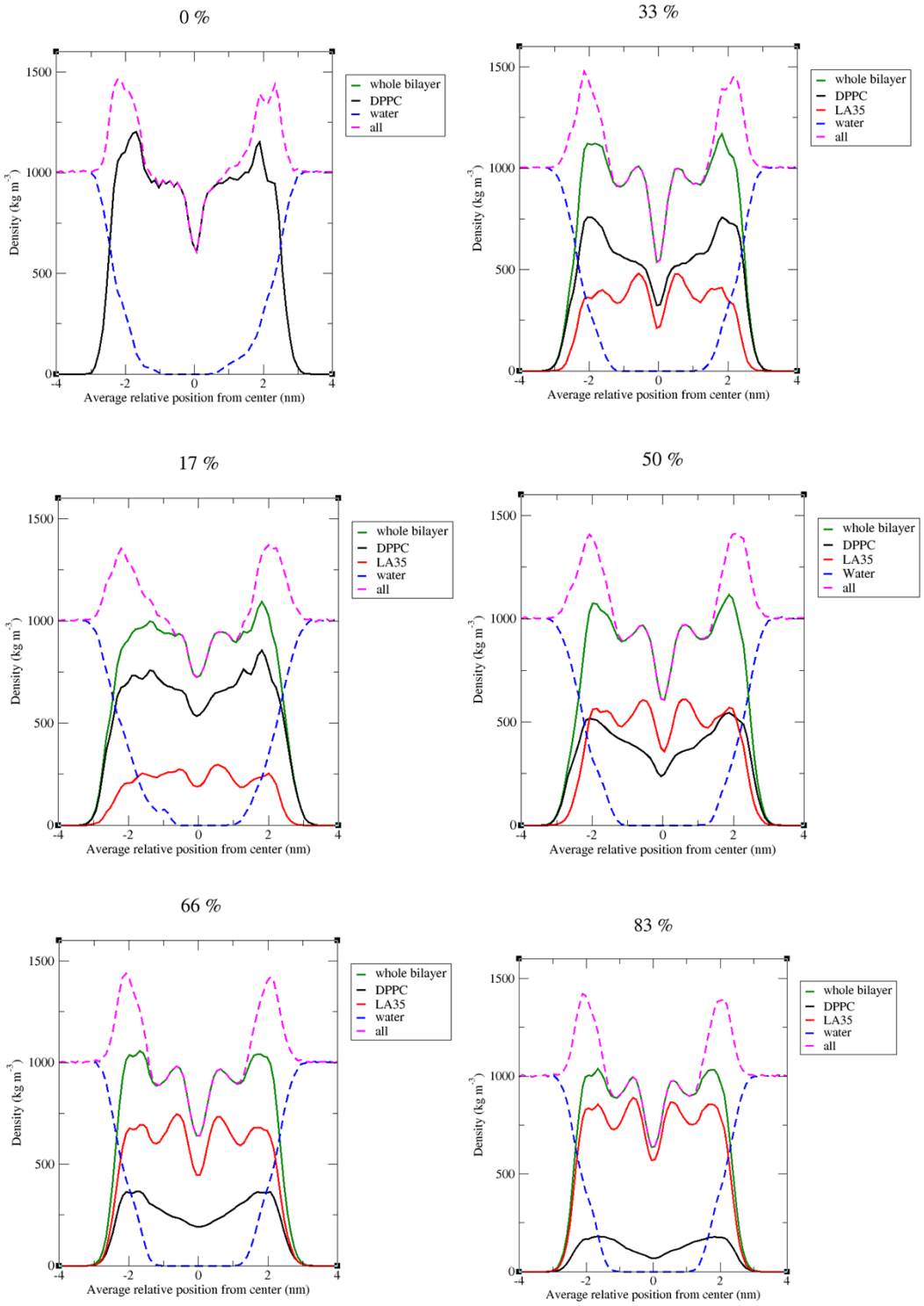

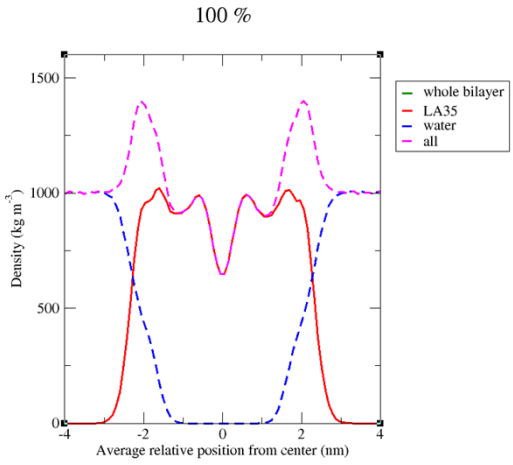

Figure S10: Density profile of LA35-DPPC bilayers with water included.

References

[S1] Piggot, T. J.; Allison, J. R.; Sessions, R. B.; Essex, J. W. On the Calculation of Acyl Chain Order Parameters from Lipid Simulations. *J. Chem. Theory Comput.* **2017**, *13* (11), 5683–5696. DOI: 10.1021/acs.jctc.7b00643.

[S2] Venable, R. M.; Brown, F. L. H.; Pastor, R. W. Mechanical Properties of Lipid Bilayers from Molecular Dynamics Simulation. *Chem. Phys. Lipids* **2015**, *192*, 60–74. DOI: 10.1016/j.chemphyslip.2015.07.014.

[S3] Hofsäss, C.; Lindahl, E.; Edholm, O. Molecular Dynamics Simulations of Phospholipid Bilayers with Cholesterol. *Biophys. J.* **2003**, *84* (4), 2192–2206.

[S4] Nagle, J. F. Experimentally Determined Tilt and Bending Moduli of Single-Component Lipid Bilayers. *Chem. Phys. Lipids* **2017**, *205*, 18–24. DOI: 10.1016/j.chemphyslip.2017.04.006.

[S5] Karmakar, S.; Raghunathan, V. Structure of Phospholipid-Cholesterol Membranes: An x-Ray Diffraction Study. *Phys. Rev. E Stat. Nonlin. Soft Matter Phys.* **2005**, *71*, 061924. DOI: 10.1103/PhysRevE.71.061924.

[S6] Marrink, S. J.; Berendsen, H. J. C. Permeation Process of Small Molecules across Lipid Membranes Studied by Molecular Dynamics Simulations. *J. Phys. Chem.* **1996**, *100* (41), 16729–16738. DOI: 10.1021/jp952956f.

[S7] MacCallum, J. L.; Tieleman, D. P. *Chapter 8 Interactions between Small Molecules and Lipid Bilayers*; Feller, S. E., Ed.; Academic Press, 2008; Vol. 60. DOI: 10.1016/S1063-5823(08)00008-2.

[S8] Róg, T.; Girych, M.; Bunker, A. Mechanistic Understanding from Molecular Dynamics in Pharmaceutical Research 2: Lipid Membrane in Drug Design. *Pharmaceuticals* **2021**, *14* (10). DOI: 10.3390/ph14101062.

[S9] Paloncýová, M.; DeVane, R.; Murch, B.; Berka, K.; Otyepka, M. Amphiphilic Drug-like Molecules Accumulate in a Membrane below the Head Group Region. *J. Phys. Chem. B* **2014**, *118* (4), 1030–1039. DOI: 10.1021/jp4112052.

[S10] Natesan, S.; Lukacova, V.; Peng, M.; Subramaniam, R.; Lynch, S.; Wang, Z.; Tandlich, R.; Balaz, S. Structure-Based Prediction of Drug Distribution across the Headgroup and Core Strata of a Phospholipid Bilayer Using Surrogate Phases. *Mol. Pharm.* **2014**, *11* (10), 3577–3595. DOI: 10.1021/mp5003366.